How to cite: *Angew. Chem. Int. Ed.* **2023**, *62*, e202304648
doi.org/10.1002/anie.202304648

CO_2 Reduction | Hot Paper

Single-Crystal to Single-Crystal Transformations: Stepwise CO_2 Insertions into Bridging Hydrides of $[(NHC)CuH]_2$ Complexes

Evan A. Patrick, Mark E. Bowden, Jeremy D. Erickson, R. Morris Bullock, and Ba L. Tran**

Abstract: Mechanistic studies of substrate insertion into dimeric $[(NHC)CuH]_2$ (NHC = N-heterocyclic carbene) complexes with two bridging hydrides have been shown to require dimer dissociation to generate transient, highly reactive (NHC)Cu–H monomers in solution. Using single-crystal to single-crystal (SC-SC) transformations, we discovered a new pathway of stepwise insertion of CO_2 into $[(NHC)CuH]_2$ without complete dissociation of the dimer. The first CO_2 insertion into dimeric $[(IPr^*OMe)CuH]_2$ (IPr*OMe = N,N′-bis(2,6-bis(diphenylmethyl)-4-methoxy-phenyl)imidazole-2-ylidene) produced a dicopper formate hydride $[(IPr^*OMe)Cu]_2(\mu\text{-}1,3\text{-}O_2CH)(\mu\text{-}H)$. A second CO_2 insertion produced a dicopper bis(formate), $[(IPr^*OMe)Cu]_2(\mu\text{-}1,3\text{-}O_2CH)(\mu\text{-}1,1\text{-}O_2CH)$, containing two different bonding modes of the bridging formate. These dicopper formate complexes are inaccessible from solution reactions since the dicopper core cleanly ruptures to monomeric complexes when dissolved in a solvent.

Introduction

The reaction of a gas and a solid organometallic complex in a single-crystal to single-crystal (SC-SC) transformation provides a crucial link between homogeneous and heterogeneous catalysis.[1] These SC-SC transformations are rare and unpredictable since small molecular changes from chemical reactions can have a detrimental effect on the crystal packing and conservation of crystallinity.[2] The rigidity of the crystal lattice in SC-SC transformations can attenuate side reactions and dissociation of weakly bound ligands, enabling structural characterization of fleeting intermediates and selective transformations that cannot be readily observed in solution.[1b,c,3]

Catalytic reduction of CO_2 has attracted intense interest for sustainable chemical production,[4] and Cu-mediated transformations of CO_2 are known for homogeneous[5] and heterogeneous systems.[4b,c,6] Copper complexes have been reported for the hydrogenation,[5a,d–f] hydroboration,[7] and hydrosilylation[8] of CO_2. Despite being recognized as a key fundamental step mediated by Cu–H complexes,[5c,9] clusters,[10] and nanoparticles,[4c] the mechanism of CO_2 insertion into Cu–H bonds remains ambiguous. The rapid rate at which CO_2 inserts into the class of dimeric complexes of $[(NHC)CuH]_2$ (NHC = IPr, 6Dipp, 7Dipp)[11] in solution to form the corresponding monomeric, two-coordinate (NHC)Cu-(κ^1-O_2CH) formate complexes[8a,12] has impeded systematic mechanistic study. Nevertheless, the insertion of CO_2 into transient monomeric Cu–H species supported by *N*-heterocyclic and cyclic alkyl amino carbene ligands has been invoked (Scheme 1A).[5a,7a] The rapid formation of (NHC)Cu(κ^1-O_2CH) is inconsistent with the rate of substrate insertion in the rate-limiting regime of Cu–H monomerization from dimeric $[(NHC)CuH]_2$ based on kinetic studies.[13] It is conceivable that a small, linear CO_2 molecule could insert into the $[Cu_2H_2]$ core of $[(NHC)CuH]_2$ *without* requiring complete dimer dissociation to form transient Cu–H monomers (Scheme 1B).

Insertions of CO_2 into metal hydride bonds in photochemical[14] and thermal reactions without necessitating formation of mononuclear metal hydrides have been reported. $L[M_3(\mu\text{-}H)_3]$ ($M = Fe^{II}$, Co^{II}, Zn^{II}; L = trianionic tris(β-diketiminate) cyclophane)[15] and Cu_nH_n (n = 3–8)

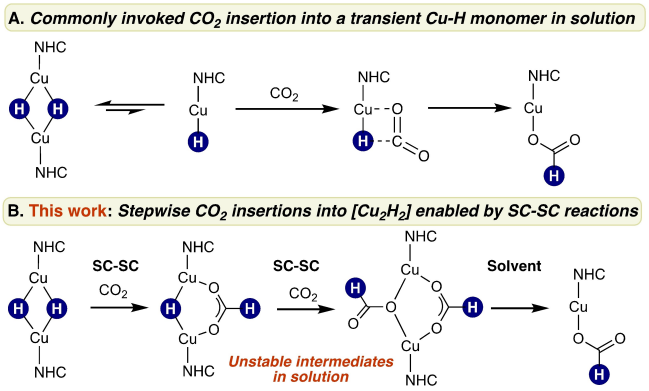

Scheme 1. Solid-gas SC-SC reactions of CO_2 and $[(NHC)CuH]_2$ enabling the characterization of unusual bridging formate intermediates that rupture in solution.

[*] Dr. E. A. Patrick, Dr. M. E. Bowden, Dr. J. D. Erickson, Dr. R. M. Bullock, Dr. B. L. Tran
Institute for Integrated Catalysis, Pacific Northwest National Laboratory
Richland, WA 99352 (USA)
E-mail: morris.bullock@pnnl.gov
ba.tran@pnnl.gov

supported by polydentate phosphine ligands have been shown to insert CO_2 into bridging hydrides to produce bridging formates.[16] The tethered tris(β-diketiminate) cyclophane ligand disfavors dissociation of the clusters to generate transient M–H monomers, in contrast to the $[(NHC)CuH]_2$ dimers that rely on their bridging hydride ligands for stability.

Insertions of unsaturated substrates into metal hydride dimers without generation of discrete hydride monomers have been experimentally observed or theoretically proposed. Specifically, insertions of nitriles or α-olefins into the bridging hydride of bimetallic complexes of Rh,[17] Fe,[18] Ca,[19] and Mg[20] to produce the corresponding bridging imido-hydride[17b,18] and bridging alkyl-hydride complexes[19c,20] have been reported. Based on DFT calculations, the insertion of 1-hexene into the $[Mg_2H_2]$ core of bimetallic $[(nacnac)MgH]_2$ in solution to produce $[(nacnac)Mg]_2(\mu\text{-hexyl})](\mu\text{-H})$ has a lower net energy barrier than the insertion of 1-hexene into monomeric (nacnac)Mg–H to produce (nacnac)Mg-hexyl.[20,21] The dimagnesium hexyl-hydride species is proposed to rapidly dissociate in solution into monomeric (nacnac)Mg-hexyl and (nacnac)Mg–H, which dimerizes to give $[(nacnac)MgH]_2$.[20]

Analogous to the dimagnesium hexyl-hydride, solvent can destabilize plausible intermediates of CO_2 insertion into $[(NHC)CuH]_2$, thereby precluding structural and spectroscopic characterization. Therefore, the detection of such unstable intermediates would necessitate the elimination of solvent. Sadighi and co-workers have structurally characterized the cationic complex of $\{[(IPr)Cu]_2(\mu\text{-}1,3\text{-}O_2CH)\}^+$,[12a] but we are unaware of neutral dicopper formate intermediates from the reactions of $[(NHC)CuH]_2$ and CO_2. We report here the SC-SC transformations for the stepwise insertion of CO_2 gas into $[(IPr^*OMe)CuH]_2$ (**1**) to produce the corresponding $[(IPr^*OMe)Cu]_2(\mu\text{-}1,3\text{-}O_2CH)(\mu\text{-H})$ (**2**) and $[(IPr^*OMe)Cu]_2(\mu\text{-}1,3\text{-}O_2CH)(\mu\text{-}1,1\text{-}O_2CH)$ (**3**) (Scheme 1, Figure 1). The isolation and reactivity of these dicopper formate species provide important mechanistic implications that improve our understanding of the insertion of CO_2 into copper-hydride dimers.

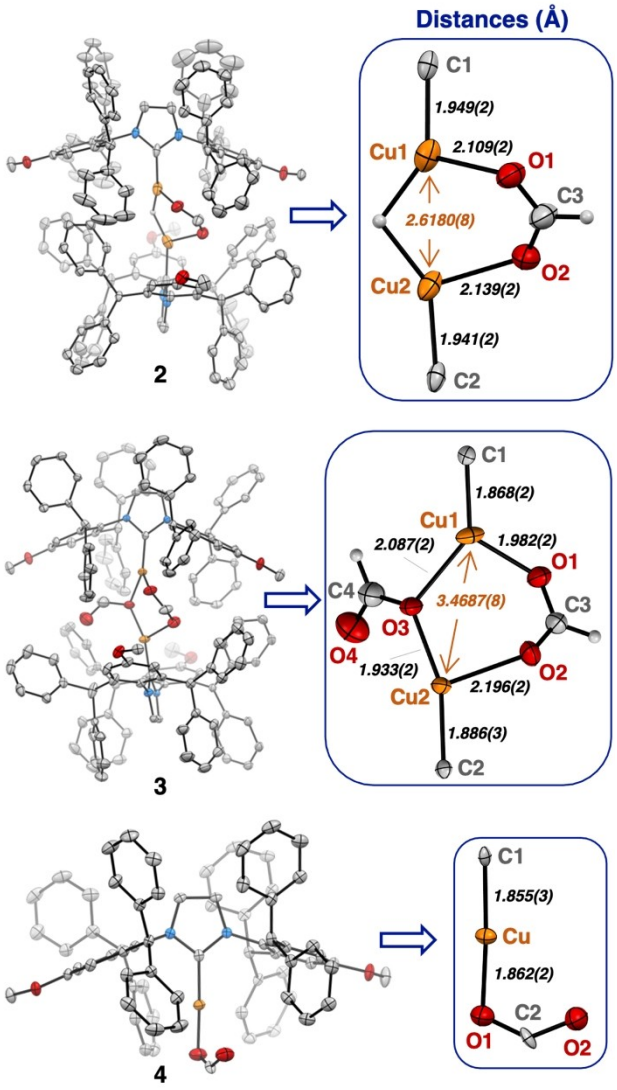

Figure 1. Molecular structures and expanded primary coordination cores of **2**, **3**, and **4** are depicted with thermal ellipsoids at 50% probability. All hydrogen atoms (except Cu–H), and co-crystallized THF have been omitted. Additional bond lengths [Å] and angles [°]: **2**, O1–C3 1.245(3), O2–C3 1.264(3). **3**, O1–C3 1.247(4), O2–C3 1.243(4), O3–C4 1.309(4), O4–C4 1.219(4), O3–Cu2–C2 160.4(1). **4**, Cu–O2 2.819(2), O1–C2 1.185(3), C2–O2 1.231(3), C1–Cu–O1 176.6(1).

Results and Discussion

Selection of $[(IPr^*OMe)CuH]_2$ for SC-SC transformations

To identify candidates for SC-SC reactions, we considered reported single crystal X-ray diffraction (SCXRD) structures of $[(NHC)CuH]_2$ complexes (NHC = IPr*Et IPr*^{t}Bu, IPr*OMe, 6Dipp, 7Dipp).[22,13] Orange single crystals of $[(IPr^*OMe)CuH]_2$ (**1**) were reliably produced from vapor diffusion of pentane into a THF solution of **1** at 25 °C, and proved suitable for SC-SC reactions. The crystal lattice of **1** contains co-crystallized THF, yet the crystals are robust. SCXRD analysis of **1** after heating at 100 °C for 24 h or under dynamic vacuum for 16 h at 25 °C did not alter the quality of the single crystals or remove the co-crystallized THF molecule from the lattice. The thermal stability of the single crystals of **1** is in stark contrast to the thermal instability of **1** in solution, for which decomposition was observed at 50 °C.

In the absence of moisture and air, the crystallinity of **1** is retained over many weeks when stored under a rigorously maintained N_2 atmosphere. For spectroscopic studies, the copper deuteride isotopologue, $[(IPr^*OMe)CuD]_2$ (**1D**), was prepared in 87% isolated yield from the reaction of (IPr*OMe)CuCl, NaO^{t}Am and $(EtO)_3SiD$. The isotopic purity of **1D** is indicated by the absence of a hydride signal at 3.92 ppm in the ^{1}H NMR spectrum, with all other resonances remaining unchanged.[23] SCXRD analysis of multiple independent crystals of **1** and **1D** shows no statistically significant differences (Figure S4).[24,25]

*The role of solvent on product identity from SC-SC and solution reactions of [(IPr*OMe)CuH]$_2$ and CO$_2$*

Exposure of orange single crystals of **1** to CO_2 (0.5 or 1.0 atm) produced colorless crystals in approximately 15 minutes (Scheme 2). The lower pressure of 0.5 atm of CO_2 yielded more crystals that remained X-ray quality compared to experiments using 1 atm of CO_2. The time required to observe the color change was not significantly altered for the two different pressures. Application of vacuum after the addition of CO_2 did not adversely affect the single-crystal quality. The SCXRD determination of the resulting colorless crystals revealed the formation of [(IPr*OMe)Cu]$_2$(1,3-μ-O_2CH)(μ-H) (**2**), as shown in Figure 1, providing unequivocal evidence for the insertion of one equivalent of CO_2 into the [CuH]$_2$ core. This binding mode of the formate ligand has been observed for {[(IPr)Cu]$_2$(1,3-μ-O_2CH)}$^+$[12a] and Cu clusters supported by polydentate phosphine ligands,[16a,b] and has been proposed as an intermediate in heterogeneously catalyzed reduction of CO_2.[16c] The distance between the Cu centers of 2.3592(8) Å in **1** has significantly increased to 2.6180(8) Å in **2**.

We anticipated that the remaining bridging hydride ligand of **2** could insert CO_2 since stepwise insertions of CO_2 into L[Fe$_3$(μ-H)$_3$],[15a,26] and of olefins into [(nacnac)CaH]$_2$,[19c] have been reported.[27] Exposing single crystals of **1** to CO_2 (1 atm) for 3 h produced (IPr*OMe)Cu]$_2$(1,3-μ-O_2CH)(1,1-μ-O_2CH) (**3**) (Figure 1), revealing two *different* formate binding modes. The 1,3-μ-O_2CH mode is common compared to that of 1,1-μ-O_2CH in bridging formate complexes.[18,28] The presence of *both* binding modes of formates has been structurally characterized for several late metal complexes.[29] In contrast to these different formate binding modes in **3**, CO_2 insertions into L[Fe$_3$(μ-H)$_3$] exclusively produced LFe$_3$(1,1-μ-O_2CH)$_3$.[15a] Interestingly, computational analysis on the first CO_2 insertion into L[Fe$_3$(μ-H)$_3$] to form L[Fe$_3$(μ-H)$_2$(1,1-μ-O_2CH)] suggests the reaction proceeds by initial formation of a 1,3-μ-O_2CH ligand followed by rearrangement to a 1,1-μ-O_2CH ligand with a computed energy barrier of 8.5 kcal mol^{-1}. The calculated ground-state structures of L[Fe$_3$(μ-H)$_2$(1,3-μ-O_2CH)] and L[Fe$_3$(μ-H)$_2$(1,1-μ-O_2CH)] differ in energy by less than 1 kcal mol^{-1}.[30]

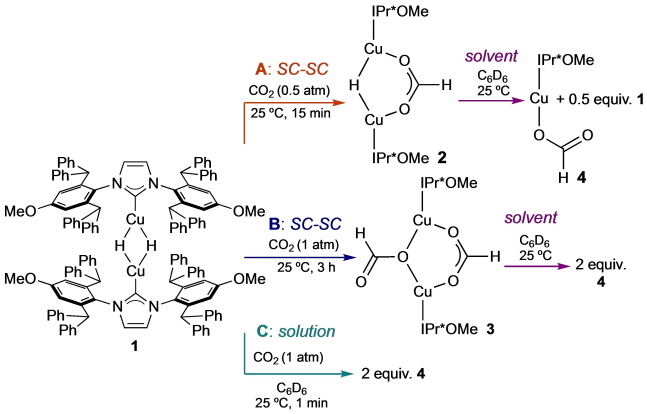

Scheme 2. Cu products from the reactions of **1** and CO_2 by sequential SC-SC then solvent (A and B) or solution reaction (C).

The unexpected observation of two distinct binding modes of formate suggests considerable change of the dicopper core after the first CO_2 insertion. DFT calculations on CO_2 insertion into a Cu$_2$(μ-H) core supported by a truncated polydentate phosphine ligand found that the ground-state structure of Cu$_2$(μ-1,3-O_2CH) is preferred over that of Cu$_2$(μ-1,1-O_2CH).[16b] Alternatively, the different binding mode may result from packing effects of the crystal lattice, in which steric environment can only accommodate formate ligands of mixed binding for the second insertion of CO_2. The double insertion of CO_2 into [(IPr*OMe)CuH]$_2$ **1** to produce *bis*(formate) complex **3** results in significant structural change as the distance between copper centers is elongated by 1.11 Å, from 2.36 Å in **1** to 3.47 Å in **3**. However, the volumes of the crystal unit cells increased by only 2.3 %.[1b] Analysis of the void space of **1** using an estimated probe radius of 1.7 Å for CO_2 did not show sufficient space in the crystal lattice to readily accommodate CO_2[31] (Figure S5). This result suggests a complex pathway by which CO_2 diffuses within the crystalline lattice towards the [Cu$_2$H$_2$] core for reaction.

Structural comparisons of **2** and **3** reveal prominent differences (Figure 1). The μ-1,3-O_2CH ligand in **2** adopts a delocalized bridging geometry, with the Cu1–O1/Cu2–O2 bond lengths differing by only 0.030 Å. In contrast, the difference in Cu1–O1 and Cu2–O2 distances in **3** is 0.214 Å. Together with the shortened Cu1-O1 and Cu2–O3 distances of 1.982(2) Å and 1.933(2) Å, respectively, and the much less bent O3–Cu2–C2 angle of 160.4° (cf. O3–Cu1–C1 at 136.8°), considerable asymmetry is observed. The average Cu-carbene bond length of **3** (1.877 Å) is also shorter than in **2** (1.945 Å), which may stem from significant electronic changes at Cu between the two complexes.

We examined the bulk samples of **3** by IR spectroscopy to analyze the stretching frequencies of the two different binding modes of the formate ligands.[32] Unfortunately, the broad, overlapping signals from the IPr*OMe ligand obscured the identification of the C–H and C–O regions corresponding to μ-1,1 and μ-1,3 formates (Figure S10). Nevertheless, we observed bands at 1628 and 1302 cm^{-1} in the expected range for the corresponding C–O asymmetric and symmetric vibration modes of a formate ligand.[32] Although the C–H region of **3** was not resolved, the isotopologue, **3D**, revealed stretches at 2108 and 2090 cm^{-1} consistent with reported C–D stretching frequencies for O_2CD ligands,[32] supporting different formate ligand environments. The C–O asymmetric and symmetric stretches could not be identified in **3D** as they were obscured by the bands from IPr*OMe.

We also investigated the effect of solvent on the stability and nuclearity of the bridging dicopper formate complexes. While the SC-SC reactions of CO_2 and [(IPr*OMe)CuH]$_2$ (**1**) retained the dicopper structure, solvent ruptures the dicopper core of **2** and **3**. Dissolution of **2** in C_6D_6 at 25 °C generates (IPr*OMe)CuO$_2$CH (**4**) and **1** (Scheme 2A, Figure S6), while dissolution of **3** produced only **4** (Scheme 2B). We have independently prepared **4** by addition of CO_2

(1 atm) to a bright orange C_6D_6 solution of **1**. In less than one minute, a colorless solution was observed, and the product **4** was verified by ^1H and ^{13}C NMR spectroscopy (Scheme 2C). The formate ligand of **4** is evidenced by signals at 8.90 ppm and 167.9 ppm in the ^1H and ^{13}C NMR spectra, respectively, and by SCXRD analysis (Figure 1). These divergent products highlight the striking differences for the reactions of CO_2 and $[(IPr^*OMe)CuH]_2$ in the solid–gas reaction compared to solution phase.

Stepwise CO_2 insertion into bulk sample of $[(IPr^*OMe)CuH]_2$

To address whether the results obtained by SCXRD analysis of the SC-SC reactions are representative of the bulk sample, we performed powder X-ray diffraction (PXRD) studies on time-dependent reactions of a single batch of **1** to produce **2**, followed by **3**. Specifically, colorless single crystals of **2** were obtained by subjecting **1** to 0.5 atm of CO_2 for 15 min, and exclusive formation of **3** was observed after treatment with 1 atm of CO_2 for 5 h. The PXRD patterns of gently ground powders of the resulting single crystals of **1**, **2**, and **3** are in excellent agreement with the those calculated from the SCXRD data (Figure 2, Figure S38–S40), with minimal differences observed across low and high angle regions. Though the overall structural perturbation between each complex is minimal, sufficient differences are observed in the PXRD patterns, allowing each structure to be distinguished, particularly in the region of 2Θ values between 9° and 11° (Figure 2).

In addition to the PXRD analysis of the SC-SC reactions, tandem solution ^1H NMR spectroscopy and PXRD studies were conducted to determine the qualitative rate of formation of **2** and **3**. The time-dependent experiments were performed by exposing the same bulk sample of single crystals of **1** to CO_2 (1 atm) at 30 min intervals, followed by PXRD and ^1H NMR spectroscopic analysis at each time increment. By ^1H NMR spectroscopy, the reaction progress was determined by quantifying the ratio of **1** and **4** over time by dissolving the solid samples in C_6D_6 (Figure S43). Separately, the PXRD measurements of each sample were modelled using a Rietveld fit, in which relative quantities of **2** and **3** were refined to obtain the best agreement between the calculated and experimental patterns (Figure S42 and S43). Solution ^1H NMR spectroscopy and PXRD analyses further support our conclusion of stepwise insertion, in which the first and second insertion of CO_2 is completed in 15 min and 2.5 h, respectively. Analogous to the SC-SC reactions, microcrystalline powders of **1** underwent a solid–gas reaction with CO_2. Exposing a pulverized powder sample of **1** to 0.5 atm of CO_2 at 25 °C for 15 min produced **2**, as evidenced by the observation of **1** and $[(IPr^*OMe)CuO_2CH]$ (**4**) in C_6D_6 by ^1H NMR spectroscopy. These results from the combination of SCXRD and PXRD studies on the SC-SC reactions strongly support the stepwise insertion of CO_2 into the $[Cu_2H_2]$ core.

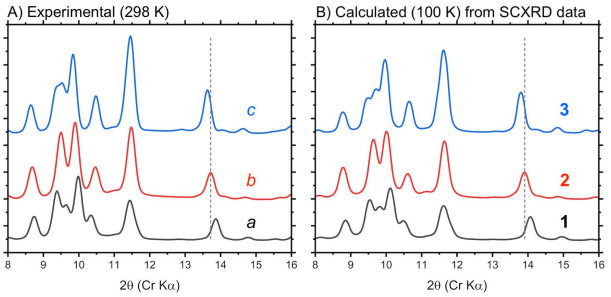

Figure 2. A) PXRD data for SC-SC conditions: (*a*) $[(IPr^*OMe)CuH]_2$ (**1**); (*b*) **1**, 0.5 atm CO_2, 15 min; (*c*) **1**, 1 atm CO_2, 5 h. B) Calculated PXRD patterns of complexes **1**, **2**, and **3**. The dashed line is provided to guide the eye towards the shift in peak position.

CO_2 insertion into the $[Cu_2H_2]$ core of $[(6Dipp)CuH]_2$

Having established that single crystals or crystalline powder of $[(IPr^*OMe)CuH]_2$ can undergo insertion of CO_2 in solid–gas reactions, we also investigated related dimeric copper hydride complexes. We examined $[(6Dipp)CuH]_2$[12b] because of its similar steric properties to the commonly used $[(IPr)CuH]_2$ with the advantage of higher solution stability to facilitate crystal growth.[8a,12a] Subjecting yellow block crystals of $[(6Dipp)CuH]_2$ (**5**) to CO_2 (1 atm) at 25 °C produced faint yellow crystals in less than 5 min (Scheme 3A). Immediate SCXRD measurement verified the formation of complex $[(6Dipp)Cu]_2(\mu\text{-}1,3\text{-}O_2CH)(\mu\text{-}H)$ (**6**). Degradation of the single crystals after CO_2 exposure produced SCXRD data suitable only for determining structural connectivity of **6** (Figure S17).

Analogous to the speciation of **2** in solution, we expect the dissolution of **6** to produce $(6Dipp)CuO_2CH$ (**8**) and $[(6Dipp)CuH]_2$ (Scheme 3A). Indeed, the ^1H NMR spectrum of **6** in THF-d_8 at 25 °C produced $[(6Dipp)CuH]_2$ (**5**) and $(6Dipp)CuO_2CH$ (**8**), as verified by resonances at 0.76 and 8.48 ppm, respectively, in the ^1H NMR spectrum (Figure S18). ^1H NMR spectroscopic characterization of $(6Dipp)CuO_2CH$ is consistent with that reported.[12b] Longer exposure of crystalline $(6Dipp)CuH]_2$ (**5**) to 1 atm CO_2 at

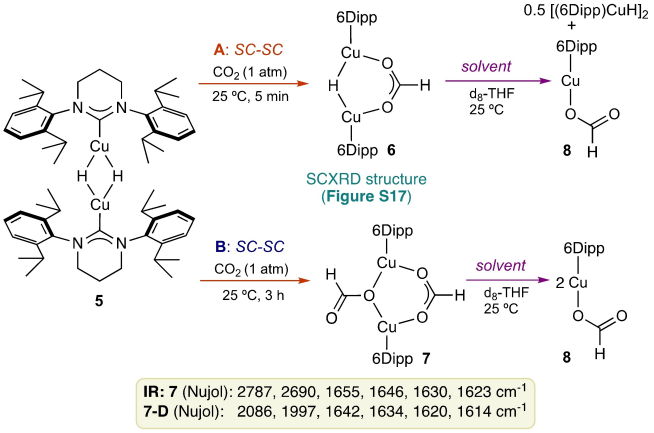

Scheme 3. Solid-gas reactions of $[(6Dipp)CuH]_2$ and CO_2 and the rupture of the dicopper formate species in solution.

25 °C for >3 h generated $[(6Dipp)Cu]_2(\mu\text{-}1,3\text{-}O_2CH)(\mu\text{-}1,1\text{-}O_2CH)$ (**7**) (Scheme 3B), which is tentatively assigned based on the structural precedent of **3**. Loss of crystallinity prevented SCXRD analysis, and we cannot definitively rule out $[(6Dipp)Cu]_2(\mu\text{-}1,3\text{-}O_2CH)_2$. The double insertion of CO_2 into **5** is supported by ^{1}H NMR and IR spectroscopic analysis. The dissolution of crystalline **7** in d_8-THF shows only $(6Dipp)CuO_2CH$ (**8**) by ^{1}H NMR spectroscopy (Scheme 3B, Figure S21), which is consistent with the exclusive formation of **4** from *bis*(formate) **3** in solution.[12b]

The IR spectrum of **7** shows two strong stretches at 2787 and 2690 cm^{-1} corresponding to the C–H modes, and four strong stretching bands at 1655, 1646, 1630, and 1623 cm^{-1} assigned to the asymmetric C–O stretching modes of the bridging formate ligands.[32] To validate that these stretches are those of the bridging formate ligands, we prepared the isotopologue $[(6Dipp)Cu]_2(\mu\text{-}1,3\text{-}O_2CD)(\mu\text{-}1,1\text{-}O_2CD)$ (**7-D**) by exposing **5-D** $[(6Dipp)CuD]_2$ to 1 atm of CO_2 for 3 h. The IR spectrum of **7-D** shows the expected shift to lower energies for the C–D stretches at 2086 and 1997 cm^{-1}, and asymmetric C–O stretches at 1642, 1634, 1620, and 1614 cm^{-1} (Figure S22).[32] In contrast, the IR spectrum of $(6Dipp)CuO_2CH$ (**8**) shows a single strong absorption at 1624 cm^{-1} for the asymmetric C–O stretch of the formate ligand (Figure S16).[32,33] A summary of the IR data of **7**, **7-D**, and **8** is provided in the Supporting Information.

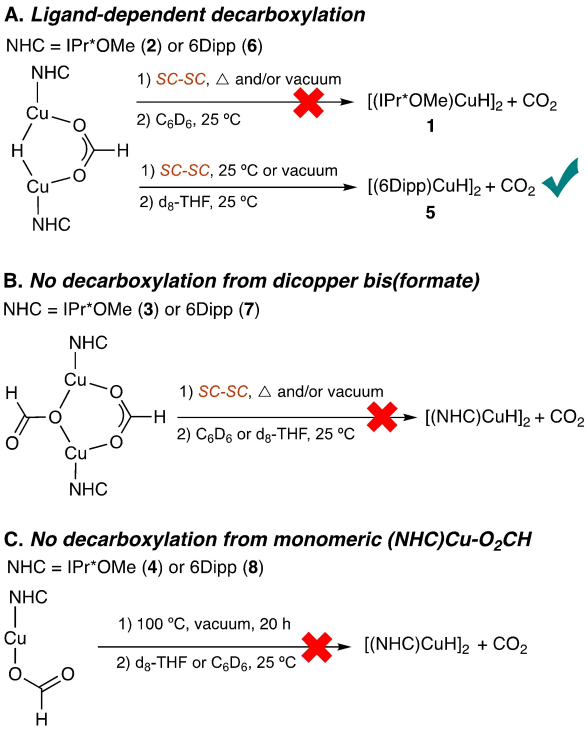

Scheme 4. Decarboxylation studies of solid dicopper formate hydride (A), dicopper *bis*(formate) (B), and monomeric copper formate (C).

Decarboxylation studies of dicopper formate hydride, dicopper bis(formate), and monomeric copper formate

The decarboxylation of dicopper complexes containing bridging μ-1,3 formate(s) to release CO_2 and regenerate Cu–H species has been observed in a stoichiometric reaction[34] and proposed in the Cu-catalyzed dehydrogenation of formic acid.[35] Therefore, we examined the decarboxylation of dicopper formate- hydride and dicopper *bis*-(formate) supported by IPr*OMe and 6Dipp ligands (Scheme 4A, B). Crystalline samples of formate hydride complex **2** and *bis*(formate) complex **3** were placed under dynamic vacuum for up to 4 days, but showed no increase in **1** by ^{1}H NMR spectroscopy in C_6D_6. These results provide no evidence for extrusion of CO_2. Heating of solids **2** and **3** at 100 °C for 3 h under vacuum gave trace conversion to unidentified products based on ^{1}H NMR spectroscopy in C_6D_6.

In stark contrast, formate hydride complex **6**, supported by the 6Dipp ligand, underwent decarboxylation under mild conditions (Scheme 4A). Colorless crystalline samples of **6** that had been stored in an open system under N_2 at room temperature overnight became yellow, characteristic of $[(6Dipp)CuH]_2$. ^{1}H NMR spectroscopic analysis of the sample before and after standing in an open vial under $N_{2(g)}$ shows an increase in **5** relative to terminal formate monomer **8**, indicating the extrusion of CO_2.

We further investigated the effect of a closed system and vacuum on the role of CO_2 on reaction equilibrium and product distribution. A sealed vial of solid **6** under $N_{2(g)}$ also turns yellow, but the product distribution in THF-d_8 remains unchanged, as indicated by ^{1}H NMR spectroscopy. This observation indicates that the extruded CO_2 is in equilibrium with respect to reinsertion into **5**. Over time CO_2 inserts into the remaining Cu–H bond of another equivalent of **6** to yield more of the thermodynamically stable *bis*(formate) **7**, which does not undergo decarboxylation, as indicated by independent control studies. The conversion of **6** to **5** occurs more rapidly when samples of **6** are placed under dynamic vacuum to remove CO_2, driving this process to completion (Figure S33).

Decarboxylation was not observed for solid samples of $(6Dipp)CuO_2CH$ (**8**) or $(IPr*OMe)CuO_2CH$ (**4**) (Scheme 4C) under dynamic vacuum for 12 h[12b] or heated at 100 °C under dynamic vacuum for 20 h (Figures S36 and S37). Dicopper formate hydride **6** has exhibited new reactivity of decarboxylation that has not been observed for monomeric (NHC)copper formate and dicopper *bis*-(formate) counterparts. Currently, we do not fully understand the role of NHC or bridging ligands for this transformation; qualitatively these results suggest the key orientation of two copper centers in close proximity for decarboxylation and a strong dependence on supporting ligand.[34]

Implications on the reaction mechanism of $[(NHC)CuH]_2$ and CO_2

The observations of CO_2 insertion into $[Cu_2H_2]$ cores without requiring complete dimer dissociation and that dicopper

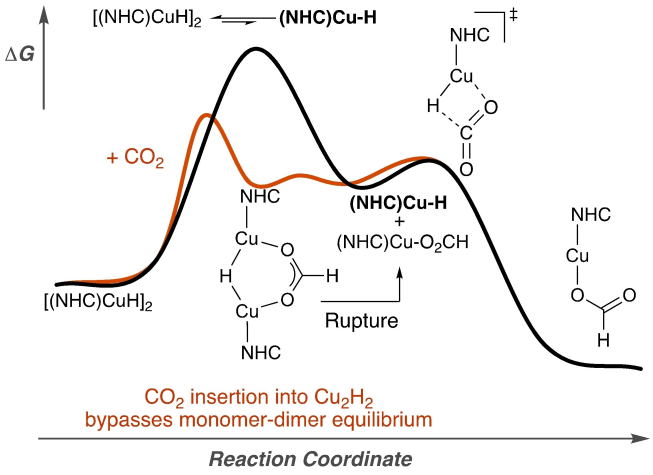

Scheme 5. Mechanistic implication of CO_2 insertion into Cu_2H_2 to override the monomer-dimer equilibrium of $[(NHC)CuH]_2$ in the solution reaction of CO_2.

formate species readily dissociate upon dissolution offer mechanistic implications on the insertion reactions of CO_2 for this class of $[(NHC)CuH]_2$ (NHC = IPr*OMe, 6Dipp) complexes. First, the faster rate of formation of formate hydride **2** compared to that of *bis*(formate) **3** may be more related to the rapid solution reaction of CO_2 and $[(NHC)CuH]_2$ to form $(NHC)CuO_2CH$. Specifically, **3** requires hours for complete formation in the solid state, whereas **2** is formed in less than 15 min, which is consistent with the rapid reactions of CO_2 and $[(NHC)CuH]_2$ (NHC = IPr*OMe, 6Dipp, 7Dipp) in solution.[12b]

Second, the facile rupture of $[(IPr*OMe)Cu]_2(1,3\text{-}\mu\text{-}O_2CH)(\mu\text{-}H)$ (**2**) into **4** and $[(IPr*OMe)CuH]_2$ in solution suggests that the first CO_2 insertion into $[(IPr*OMe)CuH]_2$ forms an unstable formate hydride dicopper (**2**) that bypasses the monomer-dimer equilibrium of $[(IPr*OMe)CuH]_2$, which typically governs the rate of substrate insertion. In the presence of excess CO_2, the resulting (IPr*OMe)CuH monomer, from the rupture of **2**, can rapidly insert CO_2 to form the second equivalent of **4** (Scheme 5). Alternatively, the (IPr*OMe)CuH monomer can dimerize to $[(IPr*OMe)CuH]_2$ and proceed in an iterative process of CO_2 insertion, rupture of **2**, and dimerization to ultimately produce the second equivalent of **4**. The high reactivity of transient (NHC)Cu–H monomers towards aldehydes and ketones likely favors the insertion of excess CO_2 into a (NHC)Cu–H monomer over dimerization to regenerate $[(NHC)CuH]_2$ (Scheme 5).[13]

Conclusion

SC-SC reactions of gaseous CO_2 and solid $[(NHC)CuH]_2$ have enabled the isolation of rare dicopper formate hydride and dicopper *bis*(formate) complexes by stepwise CO_2 insertion into bridging Cu–H bonds of $[(NHC)CuH]_2$ complexes. These dicopper intermediates are synthetically inaccessible by solution reactions of $[(NHC)CuH]_2$ and CO_2 because solvent ruptures the dicopper core into the corresponding monomeric constituents.

The rapid formation of a dicopper formate hydride species from CO_2 insertion into a dimeric $[Cu_2H_2]$ core of $[(NHC)CuH]_2$ by SC-SC reaction implies that a similar pathway is potentially operational in solution rather than requiring the formation of transient Cu–H monomers from the complete dissociation of Cu–H dimers. These observations provide experimental support of alternative insertion pathways of unsaturated substrates into metal hydride dimers without the conventionally invoked formation of a discrete monomeric metal hydride. Additionally, the isolation of dicopper formate complexes has allowed for systematic studies on the effect of nuclearity, bridging ligands, and NHC ligands on decarboxylation. The new reactivity of decarboxylation from a dicopper formate hydride is distinct from stable dicopper *bis*(formate) and monomeric formate complexes.

Lastly, the elimination of solvent and the synthetic control conferred by SC-SC reactions, which may not be accessible from solution chemistry, can potentially uncover new reactivity, mechanism, and intermediates for a range of complexes with bridging hydrides, providing an opportunity for fundamental studies at the confluence of heterogeneous, homogeneous, and gas phase chemistry.

Experimental Section

Synthetic procedures, spectroscopic characterizations, and SCXRD, PXRD parameters are provided in the Supporting Information.

Acknowledgements

This work was supported by the U.S. Department of Energy (DOE), Office of Science, Basic Energy Sciences, Chemical Sciences, Geosciences and Biosciences Division, Catalysis Science Program, FWP 47319. We thank Dr. Timothy Carroll and Dr. John Linehan for early SC-SC experiments on $[(6Dipp)CuH]_2$ and Dr. Amy L. Speelman for insight on the crystallinity of $[(IPr*OMe)CuH]_2$.

Conflict of Interest

The authors declare no conflict of interest.

Data Availability Statement

The data that support the findings of this study are available in the Supporting Information of this article.

Keywords: CO_2 Reduction · Cu Formate · Cu Hydride · N-Heterocyclic Carbenes · Single Crystal Transformation

[1] a) M. E. van der Boom, *Angew. Chem. Int. Ed.* **2011**, *50*, 11846–11848; b) S. D. Pike, A. S. Weller, *Philos. Trans. R. Soc.*

London Ser. A **2015**, *373*, 20140187; c) K. A. Reid, D. C. Powers, *Chem. Commun.* **2021**, *57*, 4993–5003; d) N. J. Coville, L. Cheng, *J. Organomet. Chem.* **1998**, *571*, 149–169.

[2] O. V. Zenkina, E. C. Keske, R. Wang, C. M. Crudden, *Angew. Chem. Int. Ed.* **2011**, *50*, 8100–8104.

[3] a) S. D. Pike, A. L. Thompson, A. G. Algarra, D. C. Apperley, S. A. Macgregor, A. S. Weller, *Science* **2012**, *337*, 1648–1651; b) A. Das, J. H. Reibenspies, Y. S. Chen, D. C. Powers, *J. Am. Chem. Soc.* **2017**, *139*, 2912–2915; c) Z. Huang, P. S. White, M. Brookhart, *Nature* **2010**, *465*, 598–601; d) C. Bianchini, E. Farnetti, M. Graziani, J. Raspar, F. Vizzat, *J. Am. Chem. Soc.* **1993**, *115*, 1753–1759; e) M. E. Bowden, B. Ginovska, M. O. Jones, A. J. Karkamkar, A. J. Ramirez-Cuesta, L. L. Daemen, G. K. Schenter, S. A. Miller, T. Repo, K. Chernichenko, N. Leick, M. B. Martinez, T. Autrey, *Inorg. Chem.* **2020**, *59*, 15295–15301.

[4] a) A. M. Appel, J. E. Bercaw, A. B. Bocarsly, H. Dobbek, D. L. DuBois, M. Dupuis, J. G. Ferry, E. Fujita, R. Hille, P. J. A. Kenis, C. A. Kerfeld, R. H. Morris, C. H. F. Peden, A. R. Portis, S. W. Ragsdale, T. B. Rauchfuss, J. N. H. Reek, L. C. Seefeldt, R. K. Thauer, G. L. Waldrop, *Chem. Rev.* **2013**, *113*, 6621–6658; b) S. Nitopi, E. Bertheussen, S. B. Scott, X. Liu, A. K. Engstfeld, S. Horch, B. Seger, I. E. L. Stephens, K. Chan, C. Hahn, J. K. Nørskov, T. F. Jaramillo, I. Chorkendorff, *Chem. Rev.* **2019**, *119*, 7610–7672; c) R. Schlögl, *Angew. Chem. Int. Ed.* **2022**, *61*, e202007397; d) M. Aresta, A. Dibenedetto, A. Angelini, *Chem. Rev.* **2014**, *114*, 1709–1742; e) H. Arakawa, M. Aresta, J. N. Armor, M. A. Barteau, E. J. Beckman, A. T. Bell, J. E. Bercaw, C. Creutz, E. Dinjus, D. A. Dixon, K. Domen, D. L. DuBois, J. Eckert, E. Fujita, D. H. Gibson, W. A. Goddard, D. W. Goodman, J. Keller, G. J. Kubas, H. H. Kung, J. E. Lyons, L. E. Manzer, T. J. Marks, K. Morokuma, K. M. Nicholas, R. Periana, L. Que, J. Rostrup-Nielson, W. M. H. Sachtler, L. D. Schmidt, A. Sen, G. A. Somorjai, P. C. Stair, B. R. Stults, W. Tumas, *Chem. Rev.* **2001**, *101*, 953–996; f) P. G. Jessop, F. Joó, C.-C. Tai, *Coord. Chem. Rev.* **2004**, *248*, 2425–2442.

[5] a) E. A. Romero, T. Zhao, R. Nakano, X. Hu, Y. Wu, R. Jazzar, G. Bertrand, *Nat. Catal.* **2018**, *1*, 743–747; b) C. M. Zall, J. C. Linehan, A. M. Appel, *ACS Catal.* **2015**, *5*, 5301–5305; c) C. M. Zall, J. C. Linehan, A. M. Appel, *J. Am. Chem. Soc.* **2016**, *138*, 9968–9977; d) R. Watari, Y. Kayaki, S.-i. Hirano, N. Matsumoto, T. Ikariya, *Adv. Synth. Catal.* **2015**, *357*, 1369–1373; e) R. Watari, S. Kuwata, Y. Kayaki, *Chem. Lett.* **2020**, *49*, 252–254; f) K. Takeuchi, Y. Tanaka, I. Tanigawa, F. Ozawa, J.-C. Choi, *Dalton Trans.* **2020**, *49*, 3630–3637.

[6] a) M. Behrens, *Angew. Chem. Int. Ed.* **2014**, *53*, 12022–12024; b) Y. Yang, S. Louisia, S. Yu, J. Jin, I. Roh, C. Chen, M. V. Fonseca Guzman, J. Feijóo, P.-C. Chen, H. Wang, C. J. Pollock, X. Huang, Y.-T. Shao, C. Wang, D. A. Muller, H. D. Abruña, P. Yang, *Nature* **2023**, *614*, 262–269.

[7] a) R. Shintani, K. Nozaki, *Organometallics* **2013**, *32*, 2459–2462; b) L. Zhang, Z. Hou, *Chem. Sci.* **2013**, *4*, 3395–3403; c) A. Hicken, A. J. P. White, M. R. Crimmin, *Angew. Chem. Int. Ed.* **2017**, *56*, 15127–15130.

[8] a) L. Zhang, J. Cheng, Z. Hou, *Chem. Commun.* **2013**, *49*, 4782–4784; b) K. Motokura, D. Kashiwame, N. Takahashi, A. Miyaji, T. Baba, *Chem. Eur. J.* **2013**, *19*, 10030–10037.

[9] M. Trivedi, A. Kumar, A. Husain, N. P. Rath, *Inorg. Chem.* **2021**, *60*, 4385–4396.

[10] a) G. Liu, P. Poths, X. Zhang, Z. Zhu, M. Marshall, M. Blankenhorn, A. N. Alexandrova, K. H. Bowen, *J. Am. Chem. Soc.* **2020**, *142*, 7930–7936; b) Y.-Z. Liu, L.-X. Jiang, X.-N. Li, L.-N. Wang, J.-J. Chen, S.-G. He, *J. Phys. Chem. C* **2018**, *122*, 19379–19384; c) Q. Tang, Y. Lee, D.-Y. Li, W. Choi, C. W. Liu, D. Lee, D.-e. Jiang, *J. Am. Chem. Soc.* **2017**, *139*, 9728–9736; d) T.-A. D. Nguyen, B. R. Goldsmith, H. T. Zaman, G. Wu, B. Peters, T. W. Hayton, *Chem. Eur. J.* **2015**, *21*, 5341–5344.

[11] IPr = 1,3-bis(2,6-diisopropylphenyl)imidazol-2-ylidene; 6Dipp = 1,3-bis(2,6-diisopropylphenyl)-tetrahydropyrimid-2-ylidene; 7Dipp = 1,3-bis(2,6-diisopropylphenyl)-tetrahydrodiazepin-2-ylidene.

[12] a) C. M. Wyss, B. K. Tate, J. Bacsa, T. G. Gray, J. P. Sadighi, *Angew. Chem. Int. Ed.* **2013**, *52*, 12920–12923; b) A. J. Jordan, C. M. Wyss, J. Bacsa, J. P. Sadighi, *Organometallics* **2016**, *35*, 613–616.

[13] a) A. L. Speelman, B. L. Tran, J. D. Erickson, M. Vasiliu, D. A. Dixon, R. M. Bullock, *Chem. Sci.* **2021**, *12*, 11495–11505; b) B. L. Tran, B. D. Neisen, A. L. Speelman, T. Gunasekara, E. S. Wiedner, R. M. Bullock, *Angew. Chem. Int. Ed.* **2020**, *59*, 8645–8653.

[14] a) R. Shimogawa, T. Takao, G.-i. Konishi, H. Suzuki, *Organometallics* **2014**, *33*, 5066–5069; b) A. Takahashi, M. Mishima, K. Nomura, A. Inagaki, *Organometallics* **2021**, *40*, 98–101.

[15] a) Y. Lee, K. J. Anderton, F. T. Sloane, D. M. Ermert, K. A. Abboud, R. Garcia-Serres, L. J. Murray, *J. Am. Chem. Soc.* **2015**, *137*, 10610–10617; b) D. M. Ermert, I. Ghiviriga, V. J. Catalano, J. Shearer, L. J. Murray, *Angew. Chem. Int. Ed.* **2015**, *54*, 7047–7050.

[16] a) K. Nakamae, M. Tanaka, B. Kure, T. Nakajima, Y. Ura, T. Tanase, *Chem. Eur. J.* **2017**, *23*, 9457–9461; b) K. Nakamae, B. Kure, T. Nakajima, Y. Ura, T. Tanase, *Chem. Asian J.* **2014**, *9*, 3106–3610; c) K. Nakamae, T. Nakajima, Y. Ura, Y. Kitagawa, T. Tanase, *Angew. Chem. Int. Ed.* **2020**, *59*, 2262–2267.

[17] a) M. D. Fryzuk, W. E. Piers, *Organometallics* **1990**, *9*, 986–998; b) M. D. Fryzuk, W. E. Piers, S. J. Rettig, *Can. J. Chem.* **1992**, *70*, 2381–2389; c) M. D. Fryzuk, W. E. Piers, *Organometallics* **1988**, *7*, 2062–2065; d) M. D. Fryzuk, W. E. Piers, *Polyhedron* **1988**, *7*, 1001–1014.

[18] Y. Yu, A. R. Sadique, J. M. Smith, T. R. Dugan, R. E. Cowley, W. W. Brennessel, C. J. Flaschenriem, E. Bill, T. R. Cundari, P. L. Holland, *J. Am. Chem. Soc.* **2008**, *130*, 6624–6638.

[19] a) A. S. S. Wilson, M. S. Hill, M. F. Mahon, C. Dinoi, L. Maron, *Science* **2017**, *358*, 1168–1171; b) A. S. S. Wilson, C. Dinoi, M. S. Hill, M. F. Mahon, L. Maron, *Angew. Chem. Int. Ed.* **2018**, *57*, 15500–15504; c) A. S. S. Wilson, M. S. Hill, M. F. Mahon, *Organometallics* **2019**, *38*, 351–360.

[20] L. Garcia, C. Dinoi, M. F. Mahon, L. Maron, M. S. Hill, *Chem. Sci.* **2019**, *10*, 8108–8118.

[21] nacnac = HC[(Me)CNAr]$_2$; Ar = 2,6-^{i}Pr-C$_6$H$_3$)].

[22] IPr*Me = N,N′-bis(2,6-bis(diphenylmethyl)-4-methylphenyl)imidazole-2-ylidene, IPr*^{t}Bu = N,N′-bis(2,6-bis(diphenylmethyl)-4-tertbutyl-phenyl)imidazole-2-ylidene, IPr*OMe = N,N′-bis(2,6-bis(diphenylmethyl)-4-methoxyphenyl)imidazole-2-ylidene.

[23] We were unable to unequivocally assign the stretching frequencies of the bridging Cu–H units of **1** and **1D** by IR spectroscopic analysis, due to the obscuring of the peaks because of overlapping in the fingerprint region Cu–H stretch and potential decreased intensity of the Cu–D stretch.

[24] Orange single crystals of [(7Dipp)CuH]$_2$, grown from toluene at −30 °C, also retained crystallinity even after 3 weeks at −30 °C, as determined by SCXRD analysis. Single-crystal quality is lost upon exposure of orange crystals of [(7Dipp)CuH]$_2$ to 0.25–1 atm of CO_2 which yielded colorless opaque solids. IR and ^{1}H NMR spectroscopic data for the solid–gas reaction are provided in the Supporting Information on pages S23–S29.

[25] Deposition Numbers 2250535 (for complex **1D**), 2250551 (for complex **2**), 2250572 (for complex **3**), and 2250573 (for complex **4**) contain the supplementary crystallographic data for this paper. These data are provided free of charge by the joint

Cambridge Crystallographic Data Centre and Fachinformationszentrum Karlsruhe Access Structures service.
[26] D. H. Hong, L. J. Murray, *Eur. J. Inorg. Chem.* **2019**, 2146–2153.
[27] Exposing single crystals of **2** to air produced a dicopper formate hydroxide complex, $[(IPr^*OMe)Cu]_2(1,3\text{-}u\text{-}O_2CH)(\mu\text{-}OH)$, as additional evidence for the second hydride remaing reactive. See connectivity XRD structure in Figure S8.
[28] F. Ritter, T. P. Spaniol, I. Douair, L. Maron, J. Okuda, *Angew. Chem. Int. Ed.* **2020**, *59*, 23335–23342.
[29] a) P. Shao, W. Zhou, Q.-L. Hong, L. Yi, L. Zheng, W. Wang, H.-X. Zhang, H. Zhang, J. Zhang, *Angew. Chem. Int. Ed.* **2021**, *60*, 16687–16692; b) T. Margossian, K. Larmier, F. Allouche, K. W. Chan, C. Copéret, *Helv. Chim. Acta* **2019**, *102*, e1800227; c) G. Feng, C. Du, L. Xiang, I. del Rosal, G. Li, X. Leng, E. Y. X. Chen, L. Maron, Y. Chen, *ACS Catal.* **2018**, *8*, 4710–4718; d) M. Kügler, J. Scholz, A. Kronz, I. Siewert, *Dalton Trans.* **2016**, *45*, 6974–6982; e) A. Rit, T. P. Spaniol, L. Maron, J. Okuda, *Angew. Chem. Int. Ed.* **2013**, *52*, 4664–4667; f) S. Schulz, T. Eisenmann, S. Schmidt, D. Bläser, U. Westphal, R. Boese, *Chem. Commun.* **2010**, *46*, 7226–7228; g) W. B. Tolman, A. Bino, S. J. Lippard, *J. Am. Chem. Soc.* **1989**, *111*, 8522–8523.
[30] D. H. Hong, R. B. Ferreira, V. J. Catalano, R. Garcia-Serres, J. Shearer, L. J. Murray, *Inorg. Chem.* **2021**, *60*, 7228–7239.
[31] E. K. Berdichevsky, V. A. Downing, R. W. Hooper, N. W. Butt, D. T. McGrath, L. J. Donnelly, V. K. Michaelis, M. J. Katz, *Inorg. Chem.* **2022**, *61*, 7970–7979.
[32] T. F. Pascher, M. Ončák, C. van der Linde, M. K. Beyer, *J. Chem. Phys.* **2020**, *153*, 184301–184311.
[33] We have independently characterized the IR data of $(6Dipp)Cu\text{–}O_2CH$, see Figure S16. The IR spectrum of $(6Dipp)Cu\text{–}O_2CH$ has also been reported by Sadighi and co-workers. See ref. [12b].
[34] J. Lücken, T. Auth, S. I. Mozzi, F. Meyer, *Inorg. Chem.* **2020**, *59*, 14347–14354.
[35] T. Nakajima, Y. Kamiryo, M. Kishimoto, K. Imai, K. Nakamae, Y. Ura, T. Tanase, *J. Am. Chem. Soc.* **2019**, *141*, 9732–8736.

Manuscript received: April 3, 2023
Accepted manuscript online: May 24, 2023
Version of record online: June 15, 2023